RSC Advances

PAPER

View Article Online
View Journal | View Issue

Cite this: *RSC Adv.*, 2023, **13**, 16651

The development of chiral metal–organic frameworks for enantioseparation of racemates†

Farzana Yasmeen, Uzma Yunus,* Moazzam H. Bhatti, Muhammad Sher and Muhammad Nadeem

Received 14th April 2023
Accepted 17th May 2023

DOI: 10.1039/d3ra02489j

rsc.li/rsc-advances

MIL-101(Cr), an achiral metal–organic framework, made up of a terephthalic acid ligand and a metal chromium ion was selected as a template. Its structural features are unsaturated Lewis acid sites that can be easily activated and it has an extremely high specific surface area, big pore size, and good thermal/chemical/water stability. This achiral framework was modified to introduce chirality within the structure to develop chiral metal–organic frameworks (CMOFs). Here, natural chiral ligands, amino acids (L-proline, L-thioproline and L-tyrosine), were selected for post synthetic modification (PSM) of **MIL-101**(Cr). This is a very simple, clean and facile methodology with respect to the reactants and reaction conditions. **CMOFs 1–3** abbreviated as **MIL-101**-L-proline (**CMOF-1**), **MIL-101**-L-thioproline (**CMOF-2**) and **MIL-101**-L-tyrosine (**CMOF-3**) were prepared by introducing L-proline, L-thioproline and L-tyrosine as chiral moieties within the framework of (Cr). These CMOFs were characterized by FTIR, PXRD, SEM, and thermo gravimetric analysis. Chirality within these **CMOFs 1–3** was established by circular dichroism (CD) and polarimetric methods. These three **CMOFs 1–3** showed enantioselectivity towards RS-ibuprofen, RS-mandelic acid and RS-1-phenylethanol to varying extents. Their enantioselectivity towards racemates was studied by chiral HPLC and polarimetry.

1. Introduction

The porous coordination networks known as metal–organic frameworks (MOFs) are created by combining metal ions and different organic linkers. These MOFs have been introduced as a large class of porous materials with extraordinary surface area, varied functionality, adaptable composition, and increased porosity. One of the profound features of MOFs is that their structure can be tuned according to applications.[1–5] Due to these properties, MOFs have recently attracted significant attention in heterogeneous catalysis, optics, biomedical applications, gas storage and especially in gas chromatography (GC) and high-performance liquid chromatography (HPLC) for the enantioseparation of racemic compounds.[6–16]

Knowledge of chirality is crucial in determining the origin of life since all chiral amino acids in enzymes are only found in their "L" form. In the field of pharmaceutical and agriculture, chiral enantiopure compounds are also important. Due to their potential use in catalysis and enantioselective separations, chiral and porous materials, like MOFs and chiral inorganic zeolites, are greatly coveted. Depending on their distinctive features, chiral metal–organic frameworks (CMOFs), in particular CMOFs with entangled systems, have demonstrated outstanding significance in recent years.[17–20] More than 30 different types of CMOFs have been created and utilised to study enantioselective adsorption so far. CMOFs face additional difficulties because of their lower stability in severe and humid environments. These problems limit the practical use of CMOFs. So, there is still dire need to explore the synthesis and applications of CMOFs.[21,22]

To the best of our knowledge, direct synthesis and post-synthetic modification are the key areas of focus when designing CMOFs for enantiomers separation. In case of direct synthesis, enantiopure ligands are usually used such as chiral bridging ligand, (*R*)-6,6-dichloro-2,2-dihydroxy-1,1-binaphthyl-4,4-bipyridine, which possess the bipyridyl group as primary and orthogonal chiral 2,2-dihydroxy as secondary functionality in their structure. A chiral 3,3′,6,6′- or 4,4′,6,6′-tetra(benzoate) ligand prepared from 1,1′-binaphthyl-2,2′-phosphoric acid has been used to prepare a porous CMOF possessing chiral pockets just like enzymes.[23,24] Many dipeptides and tripeptides also act as enantiopure ligands for the construction of CMOFs.[25] Another example of synthesis of amino acid based CMOF is development of D-his-ZIF-8. In which D-histidine is added in the reaction mixture as an enantiopure ligand which is found to be responsible of chirality in the CMOF structure.[26]

CMOFs can also be obtained from spontaneous resolution as a result of entanglement of helical molecular chains developed from achiral components. These CMOFs usually possess

Department of Chemistry, Allama Iqbal Open University, Islamabad, Pakistan. E-mail: uzma.yunus@aiou.edu.pk; uzma_yunus@yahoo.com; Tel: +9251-9057818; +9251-5975200

† Electronic supplementary information (ESI) available. See DOI: https://doi.org/10.1039/d3ra02489j

helicity of chirality. One of the best examples of three dimensional CMOFs synthesis by the spontaneous resolution is synthesis of CMOFs from achiral ligand 5-(pyridine-3-yl) isophthalic acid with different metals. Axial chirality in these CMOFs is transmitted throughout the structure.[27–29]

But, direct synthesis often relies on the self-assembly of chiral building blocks but it is usually hampered by the difficult and expensive chiral precursor synthesis processes resulting unpredictable structure and performance of the CMOFs produced.

Hence, due to the precise design of pore size/shape/surface, postsynthetic modifications (PSM) have recently been a substitute method to add chiral functions into MOFs.[30–36] Various CMOFs are synthesized by PSM of achiral MOFs.[37–43] Such as CMOF which is difficult to obtain by the simple solvothermal postsynthetic method, it is prepared alternatively by the introduction of two chiral saline moieties in UiO-68.[44] Similarly, a very facile and economically favourable method is introduced for the Zr-based MOFs by the replacement of coordinated molecules with zirconium metal in MOF-808. Formate molecules in the MOF-808 are exchanged with the chiral linker such as L-histidine, L-glutamic acid and L-tartaric acid by simply soaking the MOF-808 in salt solutions of these amino acids.[45] Other two important CMOFs, CMIL-1 and CMIL-2 are produced by the coordination of L-proline based ligands with metal centre using post synthetic strategy.[46] But, still CMOFs development faces additional difficulties in tuning the structure and properties of CMOFs. Moreover, introduction of chirality in MOFs is also very challenging in this case. Therefore, to overcome these problems, we initially selected **MIL-101** (MIL, Matérial Institut Lavoisier), as the parent achiral framework for the synthesis of **CMOFs 1–3** following this postsynthetic strategy, because it has a thermally and chemically robust structure with large pores (2.6–2.8 nm). In **MIL-101** structure, open metal coordination sites can be created to attach chiral organic ligands. The insoluble behaviour of **MIL-101** in organic solvents and water make it a suitable candidate for solid stationary phase.[47] In short, to find a simple and low-cost method for synthesizing CMOFs is challenging but also highly desired. Moreover, the right chiral additive to permit chiral transfer while maintaining the framework topology remains a difficult task.[48] For this purpose, we chose natural amino acids such as L-proline, L-thioproline and L-tyrosine as chiral ligand due to easy accessibility, availability, stability, and their coordination ability with metal centre through strong intermolecular interactions.[49] In addition, amino acids especially L-proline may also act as modulator in developing structure of CMOFs.[50–57]

Various CMOFs has been reported for enantioselective separation especially by using chromatographic techniques.[58–63] Their porous functionalities and chirality have garnered a lot of interest in enantioseparation as chiral selectors because enantioseparation play a vital role in pharmacology, molecular biology, drug delivery.[64–68] Therefore, to demonstrate a potential use of CMOFs in chiral separations, CMOFs are typically evaluated in enantioselective adsorption as chiral stationary phase. But, only a few numbers of CMOFs have been observed as chiral stationary phase in GC and LC for racemic substances. On the other hand, it is difficult to investigate further CMOFs as new stationary phase for enantioseparation because research on CMOFs employed as stationary phases using HPLC is still in its infancy.[69–71]

So, in our study, enantioselective adsorption capabilities of the three newly synthesized **CMOFs 1–3** are tried to check for separation of different racemates. Three racemic compounds, RS-ibuprofen, RS-mandelic acid and RS-1-phenylethanol have been selected as sample. For this purpose, batch experiment method and simple glass column chromatography are used as enantioseparation technique as explained in experimental section in detail.[72]

2. Experimental

2.1 Materials and methods

L-Proline, L-thioproline, L-tyrosine, RS-ibuprofen, RS-mandelic acid, RS-1-phenylethanol, $Cr(NO_3)_3 \cdot 9H_2O$, benzene dicarboxylic acid (BDC), dimethylformamide (DMF) and all organic solvents were purchased from Sigma-Aldrich. All provided solvents such as *n*-hexane, 2-propanol (IPA) and trifluoroacetic acid (TFA) were of HPLC grade. All compounds and reagents were of laboratory grade and used without further purification. Powder-X-ray diffraction (PXRD) patterns were recorded using a PANalytical X'Pert pro diffractometer with a solid-state detector using a Cu Kα source (46 kV, 35 Am, 10 divergences, receiver of 0.3 mm, anti-scatter slits, and detector) and Fourier transform infrared spectroscopy (FTIR) in ATR mode over a range of 4000 to 450 cm^{-1} using Varian FTS-800 infrared spectrophotometer. Bruker 300 MHz spectrophotometer, CHNS analysis was done by Vario MICRO cube elemental analyzer. Thermo-gravimetric analyzer, Hi-Res TGA 2950 (flow rate = 0.1 L min^{-1}) was used for TGA analysis. Other analysis such as ICP-MS was recorded using inductively coupled plasma (NexION 5000 ICP-MS) and circular dichroism studies were carried out with Jasco J-710 CD in the range of 300–220 nm, response time 0.25 sec, sensitivity 100 mdeg, resolution 1 nm, bandwidth 1.0 nm, accumulation 5 at a speed 500 nm min^{-1} in a cell length of standard 1 cm × 1 cm quartz cuvettes at 25 °C. Water was used as solvent for the preparation of samples for analysis. CMOFs were not completely dissolved in water, so very dilute water suspension were used for this purpose. The ADP400 polarimeter was used to find observed optical rotation of prepared known solutions. A sample glass tube of length 1.5 dm was used. The 3-flex surface area analyzer (Quantachrome Nova 2200e) was used to record N_2 adsorption data.

High performance liquid chromatography (HPLC) using Hitachi L-6200 and L-6000 pumps, a chiral column, CHIRALCEL® OD, 250 × 4.6 mm, 10 μm, a UV/vis detector model L-4200 Hitachi operating at (max) 268 nm, and an eluting mixture of *n*-hexane, 2-propanol and trifluoroacetic acid was used to acquire data. All measurements were done at room temperature (25 °C).

2.2 Synthesis of MIL-101 MOF

10 mmol each of $Cr(NO_3)_3 \cdot 9H_2O$ and 1,4-benzenedicarboxylic acid (10 mmol) were dissolved in 50 mL of water by sonication

(30 minutes) and then transferred to Teflon lined autoclave. The Teflon-lined steel autoclave was heated for 8 hours at 220 °C in a preheated oven. After the completion of reaction, a green-colour product was obtained which was separated by centrifugation. The product was washed three times with DMF (3 × 100 mL stirred for 20 minutes). After washing with DMF, it was stirred overnight at room temperature in chloroform and then separated by centrifugation. Finally, the green product was dried overnight at 80 °C in vacuum oven.

The FT-IR was recorded in ATR mode, ν^{-} (cm^{-1}): 3407 (O–H stretching), 1619 (COO^{-} stretching), 1398 (COO^{-} bending), 1106 (C–O stretching), 744 (C–H bending). PXRD (2ϑ): 5.9, 9.11, and 16.6.

2.3 Synthesis of CMOFs 1–3 by post synthetic method (PSM)

For the synthesis of CMOFs (**CMOF-1**, **CMOF-2** and **CMOF-3**), post synthetic modifications (PSM) of **MIL-101** was done in two steps; in the first step the activation of (3.00 mmol) of **MIL-101** was done by heating in a vacuum oven at 120 °C for 24 hours. The activated product was then cooled to room temperature and the vacuum was slowly filled with N_2 gas. In second step three **CMOFs 1–3** were developed from activated **MIL-101**. General procedure is reported here.

7.0 mmol of ligand (L-proline/L-thioproline/L-tyrosine) was dissolved in ethanol and 3.00 mmol of activated **MIL-101** was added in ligand solution. The reaction mixture was transferred in a screw capped glass vial and kept at 70 °C for three days. After the completion of reaction time, the product was recovered by centrifugation. The green product was washed three times with ethanol then with acetone and dried under vacuum at 80 °C for 8 hours before characterization as detail of synthesis is given in Scheme 1.

2.3.1 CMOF-1. FT-IR; ν^{-} (cm^{-1}): 3232 (N–H stretching), 1627 (COO^{-} asymmetric stretching), 1398 (COO^{-} bending), 1170 (C–O stretching), 736 (C–H bending). PXRD (2ϑ): 5.2, 5.9, 8.4, 9.1, 16.6. ^{1}H NMR (D_2O, 300 MHz) δ ppm: 8.2 (s, 1H), 7.66 (s, 4H), 3.59 (m, 1H), 2.78 (m, 2H), 1.65 (m, 2H).

2.3.2 CMOF-2. FT-IR; ν^{-} (cm^{-1}): 3117 (N–H stretching), 1627 (COO^{-} asymmetric stretching), 1391 (COO^{-} bending), 1027 (C–O stretching), 680 (C–S stretching), 744 (C–H bending). PXRD (2ϑ): 5.4, 5.9, 8.6, 9.3, 10.5 and 16.7. ^{1}H NMR (D_2O, 300 MHz) δ ppm: 8.2 (s, 1H), 7.66 (s, 4H), 3.59 (m, 1H), 2.78 (m, 2H), 2.1 (t, 2H), 1.65 (m, 2H).

2.3.3 CMOF-3. FT-IR; ν^{-} (cm^{-1}): 3305 (O–H stretching), 1619 (COO^{-} asymmetric stretching), 1391 (COO^{-} bending), 1012 (C–O stretching), 744 (C–H bending). PXRD (2ϑ): 5.4, 5.9, 8.5, and 9.4. ^{1}H NMR (D_2O, 300 MHz) δ ppm: 8.2 (s, 1H), 7.6 (d, 2H), 3.1 (t, 1H), 2.0 (d, 2H), 0.97 (s,2H).

2.4 Enantioseparation by CMOFs 1–3 as solid stationary phase

Enantioseparation capabilities of synthesized **CMOFs 1–3** as were examined by batch and simple glass column chromatographic methods. In these two techniques, **CMOFs 1–3** used as solid stationary phase that selectively separate the enantiomers of three racemic compounds by the procedure given below.

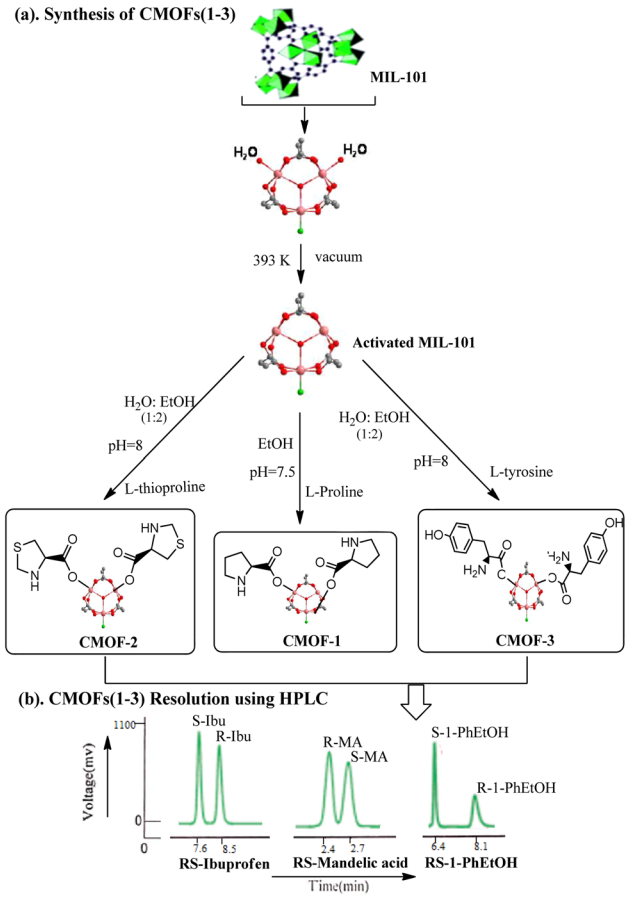

Scheme 1 Development of CMOFs 1–3 for enantioseparation.

2.4.1 Batch experiment method. This method is named as batch experiment because enantioseparation process was completed in steps. Firstly, solutions of racemates soaked in CMOFs working as chiral separator and in second step, filtration was done. Hence, firstly ethanolic solutions of these selected racemic compounds, (6.9 mg/10 mL) were soaked in 400 mg of **CMOFs 1–3** acting as solid stationary material and then in second step, after immersion of **CMOFs 1–3** in racemic solutions for 24 hours, solutions of racemates were filtered. This filterate were used for further analysis as shown in Scheme 2. The percentage of enantiomeric excess (%ee) was determined using obtained filterate for each racemate by the polarimetric and HPLC method as given in Table 3. The HPLC conditions for the determination of %ee are given in Section 2.1 in detail.

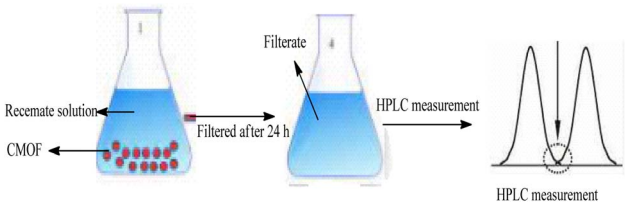

Scheme 2 Resolution of racemates by batch experiment method.

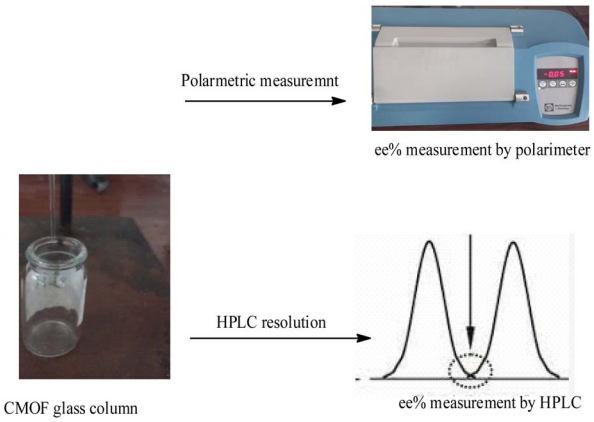

Scheme 3 Resolution of racemates by CMOFs glass columns.

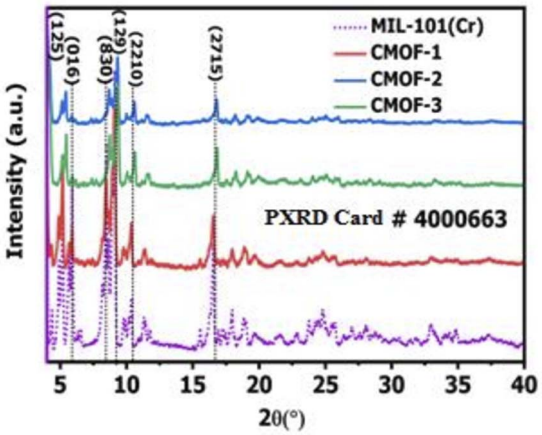

Fig. 1 PXRD spectra of MIL-101 and CMOFs 1–3.

2.4.2 Simple glass chromatography. In second method of simple glass chromatography to find the resolution ability of CMOFs, all synthesized chiral MOFs (1–3) were packed in the conventional glass column following dry method and columns were stabilized by passing acetonitrile (ACN). The **CMOFs 1–3** work as polar chiral stationary phase due to the presence of polar groups in **CMOFs 1–3**. For packing of each column, an amount of 400 mg of **CMOFs 1–3** was used. Solution of given concentration (6.9 mg mL^{-1}) of racemate was prepared in ethanol solvent and added as sample solution on the packed columns. In this method, acetonitrile was used as mobile phase because best enantioselective resolution was observed as compared to other solvent systems tried such as *n*-hexane, ethanol and *n*-hexane: ethanol. On elution, 20 fractions each of 0.5 mL volume were collected and their optical rotation was observed one by one using digital polarimeter as given in Scheme 3. Same HPLC conditions was used for determination of %ee as given in Section 2.1 but for polarimetric analysis, same solvent system was employed as that used for elution.

3. Results and discussion

MIL-101 was selected as achiral template for the post synthetically modified **MIL-101** chiral metal–organic frameworks (**CMOFs 1–3**). So, firstly, **MIL-101** was synthesized by using method described in Experimental section.[73] Various techniques were employed to confirm the structure of product *e.g.* PXRD, FTIR, ^{1}HNMR and thermo gravimetric method. All the results completely matched the reported data of **MIL-101** which confirmed the development of structure. The structural integrity of **MIL-101** was confirmed by the position and intensities of PXRD diffractions peaks. The observed PXRD pattern was found consistent with the reported pattern of **MIL-101**.[74] No additional signals were observed in the X-ray diffraction pattern as shown in Fig. 1.

After the synthesis of **MIL-101**, open coordination sites were created by removing the water molecules attached to chromium metal in the architecture. These coordination sites were used to coordinate chiral ligands which induced chirality in the structure. The activation of **MIL-101** by removing coordinated water molecules was also confirmed by FTIR analysis as given in ESI (Fig. S1†).

3.1 Characterization of synthesized CMOFs 1–3

Chiral ligands were incorporated in activated **MIL-101** and three naturally occurring amino acids were used as chiral ligands (L-proline, L-thioproline, and L-tyrosine) for the synthesis of post synthetically modified **MIL-101** chiral metal–organic frameworks as carboxylic group present in their structures possess maximum probability to coordinate with the active chromium metal node. After the development of three **CMOFs 1–3** by post synthetic modification as given in Section 2.3, all three **CMOFs 1–3** were characterized by PXRD, FTIR, BET, CD, SEM, TGA and polarimetric methods.

In PXRD analysis, same pattern for newly synthesized chiral metal–organic frameworks, **CMOF-1**, **CMOF-2** and **CMOF-3** with some decreased intensities were observed as that of **MIL-101**. It showed that basic architecture of **MIL-101** remained intact after the coordination with chiral ligands. Moreover, appearance of high intensity peaks below 10, 2ϑ-value as observed at 5.4, 5.9, 8.6, 9.3, 10.5 and 16.7 for **CMOF-1**, at 5.4, 5.9, 8.6, 9.3, 10.5 and 16.7 for **CMOF-2**.

And for **CMOF-3** at 5.4, 5.9, 8.5, 9.4 positions also indicated development of the architecture of three **CMOFs 1–3** as shown in Fig. 1.

These 2ϑ values confirmed that the structures of these CMOFs are highly porous in nature due to presence of empty spaces within the architecture of **CMOFs 1–3**.

The phase purity and crystallinity of structures is also determined which showed that decrease in crystallinity occurred by involvement of chiral ligands. The different value of decrease in crystallinity also indicated the incorporation of new chiral ligand within the architecture of **MIL-101** as given in Table 1. It is also observed that average crystallite size decreases as larger chiral moiety was introduced within the structure as calculated in **CMOF-1**, **CMOF-2** and **CMOF-3**. In case of **CMOF-3**, crystallite size becomes smaller as compared to **CMOF-1** and

Table 1 PXRD parameters for MIL-101(Cr), CMOF-1, CMOF-2, CMOF-3

Compounds	2θ (°)	FWHM (rad)	Interplanar spacing (nm)	Crystallite size (nm)	Average crystallite size (nm)	Area of crystalline peaks (nm^2)	Area of all peaks (nm^2)	Crystallinity (%)
MIL-101	5.1	0.001	1.734	95.4	33.5	25 508	41 301	61.8
	5.7	0.007	1.549	19.5				
	5.8	0.015	1.520	9.1				
	5.9	0.008	1.499	18.1				
	9.0	0.009	0.977	15.0				
	9.1	0.004	0.975	31.7				
	16.5	0.004	0.536	36.5				
	18.1	0.003	0.489	42.9				
CMOF-1	3.5	0.001	2.503	95.416	24.1	12 906	28 509	45.3
	5.2	0.007	1.712	19.460				
	5.5	0.015	1.598	9.134				
	8.5	0.004	1.042	31.676				
	9.1	0.004	0.968	36.768				
	9.2	0.003	0.960	43.312				
	16.5	0.076	0.537	1.797				
	18.0	0.094	0.494	1.460				
	18.9	0.111	0.469	1.229				
	19.7	0.129	0.451	1.061				
CMOF-2	6.4	0.056	3.677	2.157	12.3	12 300	21 895	56.2
	9.3	0.081	0.272	29.130				
	12.2	0.106	5.077	1.556				
	12.3	0.107	4.804	1.644				
	16.7	0.146	0.243	32.326				
	16.7	0.146	576.870	0.014				
	19.2	0.167	0.269	29.136				
	31.1	0.271	3.208	2.386				
	6.4	0.056	3.677	2.157				
CMOF-3	5.3	0.046	0.631	12.568	8.9	12 492	21 137	59.1
	8.7	0.076	0.242	32.755				
	9.2	0.081	0.368	21.501				
	9.2	0.081	10.824	0.732				
	9.2	0.081	10.879	0.728				
	9.2	0.081	15.887	0.498				
	19.8	0.172	8.171	0.958				
	20.8	0.181	5.813	1.344				

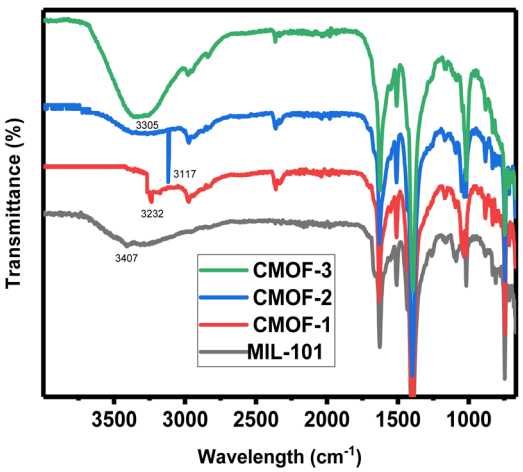

Fig. 2 FT-IR spectra of activated MIL-101 and CMOFs 1–3.

CMOF-2 due to large size of L-tyrosine as compared to L-proline and L-thioproline ligands.

FTIR analysis was done for characterization of coordination complex of chiral ligands with the activated sites (metal node) of **MIL-101** after removal of water molecules. In FTIR spectra, peaks relevant to chiral organic ligands were observed in **CMOF-1**, **CMOF-2** and **CMOF-3**. For **CMOF-1**, –NH absorption peaks appeared at 3232 cm^{-1}; 3117 for **CMOF-2** at; or **CMOF-2** but in case of **CMOF-2** this peak is somewhat sharp as compared to **CMOF-1**. In FTIR spectrum of **CMOF-3**, N–H peak is not more visible due to presence of –OH group of L-tyrosine. In **CMOF-3**, broader peak was observed as compared to **CMOF-1** and **CMOF-2** because in **CMOF-3**, free hydroxyl of L-tyrosine is present. Moreover, shifting of peaks from 1627 to 1619 cm^{-1} (COO^- asymmetric stretching vibrations) and 1398 to 1391 cm^{-1} (COO^- bending vibrations) also observed in comparison with the spectrum of achiral **MIL-101** and **CMOFs 1–3** as mentioned in Fig. 2.

For further confirmation of ligands involvement within the **CMOFs 1–3**, ^{1}HNMR technique was employed by dissociating the **CMOFs 1–3** in KOH solution. In NMR analysis, peaks at 3.59 (1H), 2.78 (2H), 1.65 (2H), 1.62 (2H) ppm appeared for **CMOF-1**, at 3.59 (1H), 2.78 (2H), 1.65 (2H) for **CMOF-2** and at 7.6 (2H), 4.7 (1H), 3.1 (2H) in case of **CMOF-3** as given in ESI (Fig. S2–S4†).

Table 2 BET analysis of CMOF-1, CMOF-2, CMOF-3

Adsorbent	BET ($m^2\ g^{-1}$)	Pore volume	Pore size (nm)
CMOF-1	Single point surface area at P/P_o = 0.200279717 = 813 $m^2\ g^{-1}$	Single point adsorption total pore volume of pores less than 78.2840 nm diameter at P/P_o = 0.974635832 = 0.89 $cm^3\ g^{-1}$	Adsorption average pore width (4 V/A by BET) = 2.21
	BET surface area = 832 $m^2\ g^{-1}$	BJH adsorption cumulative volume of pores between 1.7000 nm and 300.0000 nm diameter = 0.8714 $cm^3\ g^{-1}$	BJH adsorption average pore diameter (4 V/A) = 2.60 nm
	Langmuir surface area = 967 $m^2\ g^{-1}$	BJH desorption cumulative volume of pores between 1.7000 nm and 300.0000 nm diameter = 0.88 $cm^3\ g^{-1}$	BJH desorption average pore diameter (4 V/A) = 2.01 nm
CMOF-2	Single point surface area at P/P_o = 0.200279717 = 815 $m^2\ g^{-1}$	Single point adsorption total pore volume of pores less than 78.2840 nm diameter at P/P_o = 0.974635832 = 0.80 $cm^3\ g^{-1}$	Adsorption average pore width (4 V/A by BET) = 2.16 nm
	BET surface area = 811 $m^2\ g^{-1}$	BJH adsorption cumulative volume of pores between 1.7000 nm and 300.0000 nm diameter = 0.821 $cm^3\ g^{-1}$	BJH adsorption average pore diameter (4 V/A) = 2.19 nm
	Langmuir surface area = 887 $m^2\ g^{-1}$	BJH desorption cumulative volume of pores between 1.7000 nm and 300.0000 nm diameter = 0.814 $cm^3\ g^{-1}$	BJH desorption average pore diameter (4 V/A) = 2.1 nm
CMOF-3	Single point surface area at P/P_o = 0.200279717 = 957 $m^2\ g^{-1}$	Single point adsorption total pore volume of pores less than 78.2840 nm diameter at P/P_o = 0.974635832 = 0.79 $cm^3\ g^{-1}$	Adsorption average pore width (4 V/A by BET) = 2.18 nm
	BET surface area = 1056 $m^2\ g^{-1}$	BJH adsorption cumulative volume of pores between 1.7000 nm and 300.0000 nm diameter = 0.72 $cm^3\ g^{-1}$	BJH adsorption average pore diameter (4 V/A) = 2.31 nm
	Langmuir surface area = 1067 $m^2\ g^{-1}$	BJH desorption cumulative volume of pores between 1.7000 nm and 300.0000 nm diameter = 0.792 $cm^3\ g^{-1}$	BJH desorption average pore diameter (4 V/A) = 2.30 nm

As architectures of **CMOFs 1–3** were dissociated, some fragments of chiral ligands indicated by ^{1}HNMR spectra, but no prominent coupling was observed in ^{1}HNMR analysis.

MIL-101 was selected due to pore size 2.81 nm width and after the incorporation of L-amino acids as ligands, decrease in pore size was observed. **CMOF-1** has pore size of 2.21 nm with surface area 832 $m^2\ g^{-1}$, **CMOF-2** has pore size of 2.16 nm with surface area of 811 $m^2\ g^{-1}$ and **CMOF-3** has a pore size of 2.18 nm and surface area of 1056 $m^2\ g^{-1}$. All other parameters of BET analysis are given in detail in Table 2.

The BET analysis of these three **CMOFs 1–3** showed that these are mesoporous in nature and have the capability for adsorption. It has been observed that **CMOF-3** possess greater adsorption ability of N_2 as compared to **CMOF-1** and **CMOF-2** as shown in Fig. 3. **CMOF-1** and **CMOF-2** have comparable adsorption due to minor size difference of incorporated amino acids in these CMOFs.

The scanning electron microscopy (SEM) showed non uniformity in **MIL-101** and **CMOFs 1–3** due to some coagulation of particles as shown in Fig. 4. Moreover, particle size calculation by using SEM image showed that particles exist in the range

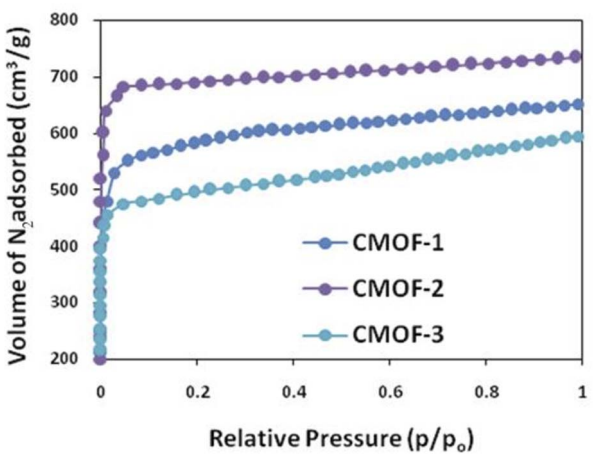

Fig. 3 BET surface area spectra of CMOFs 1–3.

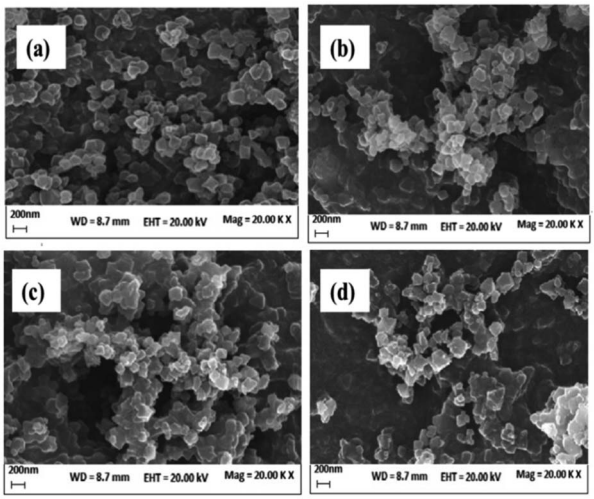

Fig. 4 SEM images of (a) MIL-101 and (b–d) CMOFs 1–3.

of 134 nm to 236 nm for **CMOF-1**, in the range of 62 nm to 255 nm for **CMOF-2** and in the range of 97 nm to 255 nm for **CMOF-3**.

The chiral nature of **CMOFs 1–3** was confirmed by polarimetric method and circular dichroism (CD). The specific optical rotation calculated for **CMOF-1** and **CMOF-2** were −38° and −40° respectively but for **CMOF-3** was −60°.

For further confirmation, CD spectrum was recorded as pure L-proline showed positive cotton effect at 222 nm in water solution but a suspension of **CMOF-1** in water shifted the value from 222 nm to 241 nm as shown in Fig. 5(a) which confirmed the coordination of L-proline ligand with chromium centre and retained the chirality, showing positive cotton effect.

In CD spectrum of **CMOF-2**, positive cotton effect at 230 nm was observed for L-thioproline in water solution and at 245 nm for **CMOF-2**. The comparison of both cures showed that shifting of ligand peak to high wavelength value from 230 nm to 245 nm with same positive cotton effect in case of **CMOF-2** which confirmed the incorporation of ligand within the structure in Fig. 5(b).

In CD spectrum of **CMOF-3**, positive cotton effect at 271 nm was observed for L-tyrosine ligand in water solution and at 287 nm for **CMOF-3**.

The comparison of both curves showed that shifting of ligand peak to high wavelength value from 271 nm to 287 nm with same positive cotton effect in case of **CMOF-3** which confirmed presence of chirality due to attachment of chiral ligand within the structure as indicated in Fig. 5(c).

3.2 Determination of CMOFs 1–3 purity and stability

After the complete characterization of CMOFs, their purity and stability was also examined because purity and stability of architecture is highly concerned while performing enantioseparation. The stability of **CMOFs 1–3** was determined by thermal gravimetric measurements. The results of TGA also justify the purity of **MIL-101** and synthesized **CMOFs 1–3**. TGA analysis showed firstly ethanol molecules removal at 82 °C and

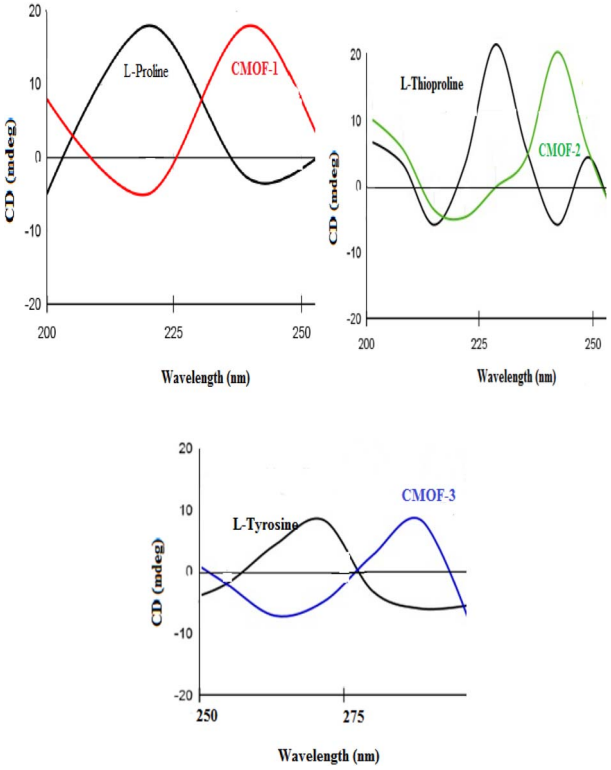

Fig. 5 CD spectra of chiral ligands and CMOFs 1–3.

then trapped water molecules 12% removal occurred at 243 °C. The removal of water molecules at this high temperature of 243 °C indicated that these water molecules have very strong coordination with the metal centre. The further weight loss of chiral ligands and benzene dicarboxylic acid ligand was observed in the temperature range of 378 °C to 484 °C.

At the end, 24% of Cr_2O_3 remained as residue at 600 °C in case of **CMOFs 1–3** as given Fig. 6. The FTIR spectra also clarify the purity of **CMOFs 1–3** because no extra peaks appeared in FTIR spectra of **CMOFs 1–3**.

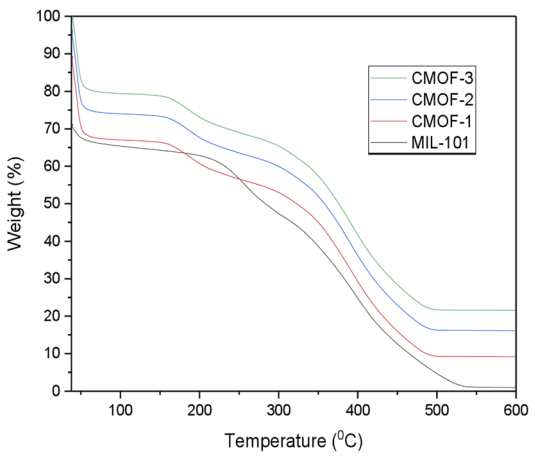

Fig. 6 TGA spectra of MIL-101 and CMOFs 1–3.

3.3 Enantioseparations studies by synthesized CMOFs 1–3

Resolution of racemates by using chiral stationary phases is considered one of the best strategies to get enantiopure compounds. For this purpose, porous CMOFs having maximum stability in humid environment are very fascinating material as chiral stationary phase. The enantioselective properties of synthesized **CMOFs 1–3** as chiral stationary phase were examined by using two methods, batch experiment method and simple glass chromatography. Racemate such as RS-ibuprofen (IBU), RS-mandelic acid (MA) and RS-1-phenylethanol (PhE-tOH) were selected to find the enantioselectivities of synthesized **CMOFs 1–3** depending on easy availability, high thermal stability, possible accessible molecular size, or suitable minimum kinetic diameter (MKD) and the polar nature of these compounds due to presence of polar functional groups. The main reason of selection of these polar groups containing racemate is their maximum interactions possibility with chiral stationary phase as **CMOFs 1–3** are also polar in nature.

Batch experiment was performed to calculate enantioselectivities of **CMOFs 1–3** as given in Scheme 2. Second method of simple glass column chromatography was also employed to check the enantioselective nature of **CMOFs 1–3** however; best results were obtained by batch experiment.

It was observed that best resolution was shown by RS-1-phenylethanol as compared to RS-ibuprofen and RS-mandelic acid in case of all three synthesized **CMOFs 1–3**. To evaluate the enantioselectivities of **CMOFs 1–3** for RS-1-phenylethanol, firstly HPLC analysis for racemic solution was done. The enantiomeric excess (%ee) value was calculated for racemate and for **CMOFs 1–3** one by one using chiral HPLC and compared their values as shown in ESI (Fig. S5–S7†).

To explain the mechanism of chiral separation by these **CMOFs 1–3** used as chiral stationary phase employed both in batch experiment and glass chromatography, nature of chiral points within the pockets of CMOFs stationary phases was studied. The FTIR spectra of these CMOFs clearly showed that amino group in the structure is available for interactions with the incoming chiral moieties as given in Fig. 2. As a result of these interactions, diastereomeric relationship may develop. The HPLC results as given in ESI† proved that these interactions of chiral points present within the CMOFs stationary phases with chiral groups exist in racemates are very weak which develop temporarily then detach resulting elution of one enantiomer than the other one.

In case of enantioseparation of 1-phenylethanol, the enhanced enantioselective ability for **CMOFs 1–3** may be attributed to the small volume of RS-1-phenylethanol (125.45 cubic angstrom) and optimum orientation of hydroxyl group of 1-phenylethanol with the functional groups present in the structure of **CMOFs 1–3**.[75–79] **CMOF-1** and **CMOF-2** resolved the enantiomers of 1-phenylethanol with 19% ee value.

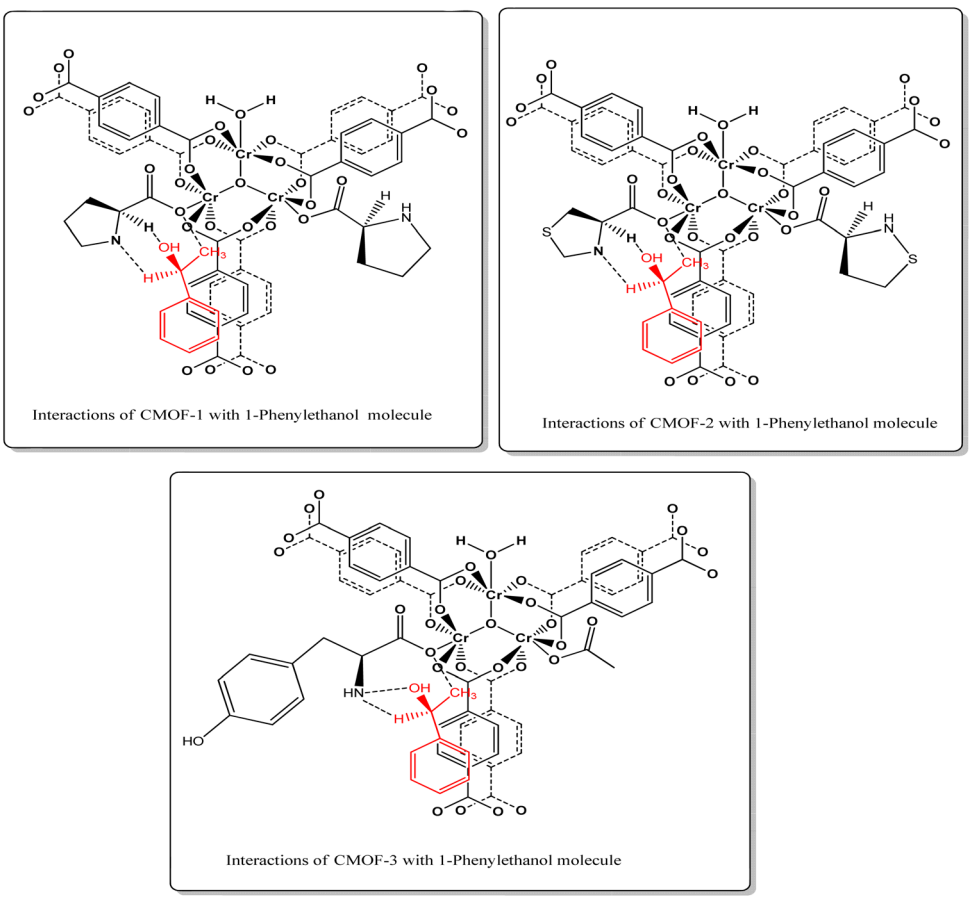

Fig. 7 Three-points electrostatic interactions illustrated by the dotted lines between the chiral centres of **CMOFs 1–3** and 1-phenylethanol.

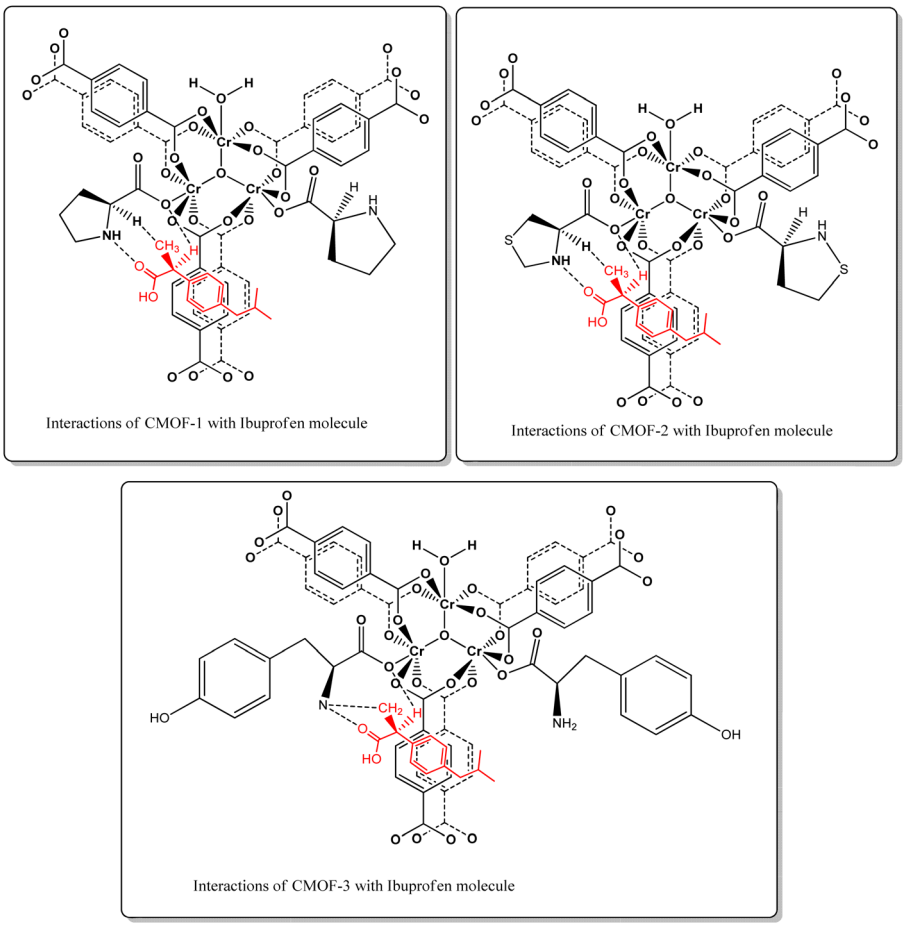

Fig. 8 Three-points electrostatic interactions illustrated by the dotted lines between the chiral centres of CMOFs 1–3 and ibuprofen molecule.

Whereas **CMOF-3** showed greater enantioselectivities for this racemic compound with 46% enantiomeric excess as shown in HPLC spectrum which may be attributed to maximum interactions with free hydroxyl group available in **CMOF-3** however its exact mechanism is still under research. Dalgliesh's three-point interaction theory may also explain this enantioselective recognition as this theory states that one enantiomer of a chiral compound should interact with at least three points around the chiral centre of the adsorbent *via* hydrogen bonding, dipole–dipole interactions, or other intermolecular forces, resulting in a transient diastereomeric interaction that leads to chiral recognition.[80] As these interactions, most probably three-point hydrogen bonding and other intermolecular interactions strongly occurs in case of 1-phenylethanol and L-tyrosine ligand causing high enantioselectivity as compared to other two **CMOFs 1–2** as given in Fig. 7. This theory also supports the retention of chirality while performing the enantioseparation by **CMOFs 1–3**.

CMOFs 1–3 also showed enantioselective adsorption for other two racemate such as RS-ibuprofen and RS-mandelic acid but showed best resolution for RS-ibuprofen as given in ESI.†

CMOF-1 and **CMOF-2** resolved enantiomers of RS-ibuprofen with 18% enantiomeric excess, however **CMOF-3** showed 15% enantiomeric excess. As ibuprofen possess 7.4 Å minimum

Table 3 Enantioseparations results for different racemic compounds[a]

Enantiomers	CMOF-1	CMOF-2	CMOF-3
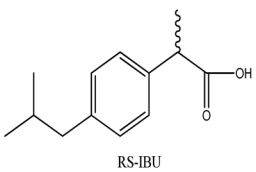 RS-IBU	18%	18%	15%
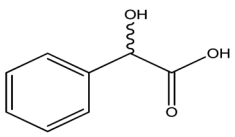 RS-MA	6%	5%	11%
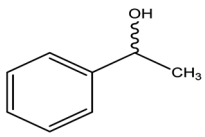 RS-1-PhEtOH	19%	19%	46%

[a] The %ee value was calculated by the formula, $\%ee = [(R - S)/(R + S) \times 100]$.

Table 4 Comparison of properties of incorporated ligands (1–3) and CMOFs 1–3 with enantioseparations

	Molar volume of ligand (cm^3)	Polar surface area of ligand (A^2)	BET surface area of CMOF ($m^2\ g^{-1}$)	% ee for racemates		
				IBU	MA	1-PhEtOH
CMOF-1	97.0 ± 3.0	49	832	18	6	19
CMOF-2	96.5 ± 3.0	75	811	18	5	19
CMOF-3	135.9 ± 3.0	84	1056	15	11	46

kinetic diameter (MKD) as calculated by Gaussian software which is accessible molecular size for these porous **CMOFs 1–3**.

Moreover, the possible interactions of RS-ibuprofen with three synthesized **CMOFs 1–3** according to three-point theory are illustrated in Fig. 8.

CMOFs 1–3 enantioselectivity for RS-mandelic acid was very lethargic with 5–11% enantiomeric excess.

It means that presence of number of functional groups and size of racemic compounds affects the enantioselectivities of **CMOFs 1–3**. The presence of two hydroxyl groups in the mandelic acid may cause steric hindrance resulting less enantioselectivity.

It is also observed that various properties of ligands incorporated in **CMOFs 1–3** affected the enantioselectivities of **CMOFs 1–3** as given in Table 4. The polar surface area of ligand and BET surface area of resultant CMOF greatly has determined the enantioselectivities of **CMOFs 1–3**.

The polar groups present in ligands interact with the functional group of racemic molecules and promote enantioseparation. It also showed by the results that increasing BET surface area of **CMOFs 1–3** also increased enantioselectivity for selected racemic molecules.

As polar surface area of racemic ibuprofen and racemic 1-PhEtOH found in the range of 20–37 A^2, so **CMOF-1** showed comparable %ee value (18–19%) but racemic mandelic acid possess 58 A^2 polar surface area and resulted poor enantioseparation (6%).

In case of **CMOF-2**, molar volume is approximately similar but polar surface area increased due to presence of sulphur group. Sulphur didn't interact efficiently with functional groups of racemate, that's why **CMOF-2** also has comparably similar enantioseparation values as given in Table 3.

CMOF-3 has maximum polar surface area, so showed best resolution for all three racemic molecules especially for 1-PhEtOH (%ee, 46%). The %ee value also showed that.

Orientation of functional groups also enhanced the enantioselectivity as shown in Fig. 7. In case of racemic ibuprofen and racemic mandelic acid, carboxyl group may create hindrance leading less enantioseparation as compared to 1-PhEtOH.

In all these **CMOFs 1–3**, **CMOF-3** showed best resolution for 1-phenylethanol with 46% enantiomeric excess. Moreover, enantioselectivity of three synthesized **CMOFs 1–3** also compared with other physical properties especially BET surface area of **CMOFs 1–3**.

The retention of chirality in **CMOFs 1–3** also observed by CD spectra, as no change in sign of cotton effect appeared as given in Fig. 5.

Moreover, these CMOFs are prepared in clean environment and showed maximum stability in humid conditions.[81] These CMOFs also showed improved results for 1-phenylethanol as previously synthesized Zr based CMOFs using same enantioseparation strategy. The previously reported Zr based CMOFs also derived from naturally occurring amino acids and MOF-808, however their enantioselective capability towards these racemates was not attractive as shown by the present work. So, these **CMOFs 1–3** works as good stationary material as compared to previously reported following the same enantioseparation methodology.

4. Conclusions

In conclusion, we have synthesized new chiral materials by the post synthetic modification of **MIL-101**(Cr), which can be employed for the enantioseparation of racemic compounds. All these three **CMOFs 1–3** were prepared by the post synthetic strategy, which is very easy, clean, and economically favourable method because naturally occurring amino acids have used as ligands under mild conditions. The enantioselective properties of these CMOFs were evaluated by selecting RS-ibuprofen, RS-mandelic acid and RS-1-phenylethanol racemate. For this purpose, batch experiment method and simple glass column chromatography was used, and results were further confirmed by using polarimetric and HPLC techniques. In all these **CMOFs 1–3**, **CMOF-3** showed best resolution for 1-phenylethanol with 46% enantiomeric excess. Moreover, enantioselectivity of three synthesized **CMOFs 1–3** also compared with other physical properties especially BET surface area of **CMOFs 1–3**.

Conflicts of interest

There are no conflicts to declare.

Acknowledgements

The Authors would like to thank Allama Iqbal Open University, Islamabad, Pakistan for providing research facilities.

Notes and references

1 K. K. Gangu, S. Maddila, S. B. Mukkamala and S. B. Jonnalagadda, *Inorg. Chim. Acta*, 2016, **446**, 61–74.
2 K. K. Gangu and S. B. Jonnalagadda, *Front. Sci. Ser.*, 2021, **9**, 747615.
3 A. Rubab, A. Altaf, S. Ishtiaq and M. Sohail, *Nano Sci*, 2022, 106–132.
4 D. Zhao, W. Zhang, Z. Wu and H. Xu, *Front. Chem.*, 2021, **9**, 834171.

5 A. Karmakar, A. V. Desai and S. K. Ghosh, *Coord. Chem. Rev.*, 2016, **307**, 313–341.
6 X. J. Hu, Z. X. Li, H. Xue, X. Huang, R. Cao and T. F. Liu, *CCS Chem.*, 2020, **2**(1), 616–622.
7 Y. Keum, S. Park, Y. P. Chen and J. Park, *Angew. Chem., Int. Ed.*, 2018, **130**(45), 15068–15072.
8 F. Rouhani, F. Rafizadeh-Masuleh and A. Morsali, *J. Am. Chem. Soc.*, 2019, **141**(28), 11173–11182.
9 Y. Jiao, J. Yin, H. He, X. Peng, Q. GAO and C. Duan, *J. Am. Chem. Soc.*, 2018, **140**(18), 5882–5885.
10 R. B. Lin, S. Xiang, H. Xing, W. Zhou and B. Chen, *Coord. Chem. Rev.*, 2019, **378**, 87–103.
11 S. Yuan, L. Feng, K. Wang, J. Pang, M. Bosch, C. Lollar and H. C. Zhou, *Adv. Mater.*, 2018, **30**(37), 1704303.
12 S. M. Xie, M. Zhang, Z. X. Fei and L. M. Yuan, *J. Chromatogr. A*, 2014, **1363**, 137–143.
13 L. Li, J. D. Yi, Z. B. Fang, X. S. Wang, N. Liu, Y. N. Chen and R. Cao, *Chem. Mater.*, 2019, **31**(18), 7584–7589.
14 G. Huang, L. Yang, Q. Yin, Z. B. Fang, X. J. Hu, A. A. Zhang and R. Cao, *Angew. Chem., Int. Ed.*, 2020, **59**(11), 4385–4390.
15 C. Zhuo, Y. Wen, S. Hu, T. Sheng, R. Fu, Z. Xue and X. Wu, *Inorg. Chem.*, 2017, **56**(11), 6275–6280.
16 Z. G. Gu, C. Zhan, J. Zhang and X. Bu, *Chem. Soc. Rev.*, 2016, **45**(11), 3122–3144.
17 S. Tanase-Grecea, E. Sharon, W. Sander and D. David, *Chem.–A Eur. J.*, 2020, **26**.
18 F. Wang, H.-R. Fu and J. Zhang, *Cryst. Growth Des.*, 2015, **15**(4), 1568–1571.
19 G.-L. Wen, G. P. Yang, P. Liu, B. Liu and Y. Y. Wang, *Inorg. Chem. Commun.*, 2018, **94**, 104–107.
20 M. Zhou, D. Yan, Y. Dong, X. He and Y. Xu, *Inorg. Chem.*, 2017, **56**(15), 9036–9043.
21 Z.-G. Gu, S. Grosjean, S. Brase, C. Woll and L. Heinke, *Chem. Commun.*, 2015, **51**(43), 8998–9001.
22 X. Chen, H. Jiang, B. Hou, W. Gong, Y. Liu and Y. Cui, *J. Am. Chem. Soc.*, 2017, **139**(38), 13476–13482.
23 C.-D. Wu, A. Hu, L. Zhang and W. Lin, *J. Am. Chem. Soc.*, 2005, **127**(25), 8940–8941.
24 M. Zheng, Y. Liu, C. Wang, S. Liu and W. Lin, *Chem. Sci.*, 2012, **3**(8), 2623–2627.
25 J. Bonnefoy, A. Legrand, E. A. Quadrelli, J. Canivet and D. Farrusseng, *J. Am. Chem. Soc.*, 2015, **137**(29), 9409–9416.
26 J. Zhao, H. Li, Y. Han, R. Li, X. Ding, X. Feng and B. Wang, *J. Mat. Chem. A*, 2015, **3**(23), 12145–12148.
27 T. Ezuhara, K. Endo and Y. Aoyama, *J. Am. Chem. Soc.*, 1999, **121**(14), 3279–3283.
28 X. Tan, J. Zhan, J. Zhang, L. Jiang, M. Pan and C.-Y. Su, *CrystEngComm*, 2012, **14**(1), 63–66.
29 B. Gil-Hernández, H. A. Höppe, J. K. Vieth, J. Sanchiz and C. Janiak, *Chem. Comm.*, 2010, **46**(43), 8270–8272.
30 Y. Liu, W. Xuan and Y. Cui, *Adv. Mater.*, 2010, **22**(37), 4112–4135.
31 Y. Lu, H. Zhang, J. Y. Chan, R. Ou, H. Zhu, M. Forsyth and H. Wang, *Angew. Chem., Int. Ed.*, 2019, **131**(47), 17084–17091.
32 W. T. Kou, C. X. Yang and X. P. Yan, *J. Mat. Chem. A*, 2018, **6**(37), 17861–17866.
33 M. Xue, B. Li, S. Qiu and B. Chen, *Mat. Today*, 2016, **19**(9), 503–515.
34 X. Feng, H. S. Jena, K. Leus, G. Wang, J. Ouwehand and P. Van Der Voort, *J. Catal.*, 2018, **365**, 36–42.
35 W.-T. Kou, C.-X. Yang and X.-P. Yan, *J. Mater. Chem. A*, 2018, **6**(37), 17861–17866.
36 Z. Hu, Y. Peng, Y. Gao, Y. Qian, S. Ying and D. Yuan, *Chem. Mater.*, 2016, **28**(8), 2659–2667.
37 X. Ma, Y. Guo, L. Zhang, K. Wang, A. Yu, S. Zhang and G. Ouyang, *Talanta*, 2022, **239**, 123143.
38 S. Li, Y. Zhou and B. Yan, *Inorg. Chem.*, 2022, **61**(25), 9615–9622.
39 M. Ma, C. Jiahuan, H. Liu, Z. Huang, H. Fuhong, L. Quanliang and X. Yuan, *Nanoscale*, 2022, **14**, 13405–13427.
40 A. Gheorghe, B. Strudwick, D. M. Dawson, S. E. Ashbrook, S. Woutersen, D. Dubbelda and S. Tanase, *Chem.–A Eur. J.*, 2020, **26**(61), 13957–13965.
41 K. Berijani and A. Morsali, *Inorg. Chem.*, 2020, **60**(1), 206–218.
42 W. T. Kou, C. X. Yang and X. P. Yan, *J. Mater. Chem. A*, 2018, **6**(37), 17861–17866.
43 C. Tan, X. Han, Z. Li, Y. Liu and Y. Cui, *J. Am. Chem. Soc.*, 2018, **140**(47), 16229–16236.
44 C. Tan, X. Han, Z. Li, Y. Liu and Y. Cui, *J. Am. Chem. Soc.*, 2018, **140**(47), 16229–16236.
45 X. J. Hu, G. Huang, S. Zhang, Z. B. Fang, T. F. Liu and R. Cao, *Chem. Comm.*, 2020, **56**(54), 7459–7462.
46 M. Banerjee, S. Das, M. Yoon, H. J. Choi, M. H. Hyun, S. M. Park and K. Kim, *J. Am. Chem. Soc.*, 2009, **131**(22), 7524–7525.
47 G. Férey, C. Mellot-Draznieks, C. Serre, F. Millange, J. Dutour, S. Surblé and I. Margiolaki, *Science*, 2005, **309**(5743), 2040–2042.
48 R. A. Sheldon, *Chirotechnology: Industrial Syn. of Optically Active Compounds*, CRC press, 1993.
49 R. E. Morris and X. Bu, *Nat. Chem.*, 2010, **2**(5), 353–361.
50 P. Deria, J. E. Mondloch, E. Tylianakis, P. Ghosh, W. Bury, R. Q. Snurr and O. K. Farha, *J. Am. Chem. Soc.*, 2013, **135**(45), 16801–16804.
51 G. Lidi, H. Xingfang, Q. Shili, C. Hongtao, Z. Xuan and W. Bingbing, *RSC Adv.*, 2022, **12**(10), 6063–6075.
52 B. Ding, M. B. Solomon, C. F. Leong and D. M. D'Alessandro, *Coord. Chem. Rev.*, 2021, **439**, 213891.
53 R. K. Gupta, M. Riaz, M. Ashfaq, Z. Y. Gao, R. S. Varma, D. C. Li and D. Sun, *Coord. Chem. Rev.*, 2022, **464**, 214558.
54 Q. Shili, S. Yangyang, H. Xudong, C. Hongtao, G. Lidi and H. Zhongyu, *RSC Adv.*, 2021, **11**(59), 37584–37594.
55 C. E. Bien, Z. Cai and C. R. Wade, *Inorg. Chem.*, 2021, **60**(16), 11784–11794.
56 M. Banerjee, S. Das, M. Yoon, H. J. Choi, M. H. Hyun and K. Park, *J. Am. Chem. Soc.*, 2009, **131**(22), 7524–7525.
57 S. M. Xie, Z. J. Zhang, Z. Y. Wang and L. M. Yuan, *J. Am. Chem. Soc.*, 2011, **133**(31), 11892–11895.
58 A. L. Nuzhdin, D. N. Dybtsev, K. P. Bryliakov, E. P. Talsi and V. P. Fedin, *J. Am. Chem. Soc.*, 2007, **129**(43), 12958–12959.

59 M. Padmanaban, P. Müller, C. Lieder, K. Gedrich, R. Grünker, V. Bon and S. Kaskel, *Chem. Commun.*, 2011, **47**(44), 12089–12091.
60 K. Tanaka, T. Muraoka, D. Hirayama and A. Ohnish, *Chem. Commun.*, 2012, **48**(68), 8577–8579.
61 J. K. Chen, N. Y. Xu, P. Guo, B. J. Wang, J. H. Zhang, S. M. Xie and L. M. Yuan, *J. Sep. Sci.*, 2021, **44**(21), 3976–3985.
62 Y. Zhang, X. Jin, X. Ma and Y. Wang, *Anal. Methods*, 2021, **13**(1), 8–33.
63 *Enantiomer separation: fundamentals and practical methods*, ed. F. Toda, Springer Science and Business Media, 2007.
64 T. A. Goetjen, J. Liu, Y. Wu, J. Sui, X. Zhang and J. T. Hupp, *Chem. Commun.*, 2020, **56**(72), 10409–10418.
65 J. Li, Y. Ren, C. Qi and H. Jiang, *Dalton Trans.*, 2017, **46**(24), 7821–7832.
66 B. Shen, Y. Kim and M. Lee, *Adv. Mater.*, 2020, **32**(41), 1905669.
67 C.-X. Yang and X.-P. Yan, *Anal. Chem.*, 2011, **83**(18), 7144–7150.
68 Z.-L. Fang, S. R. Zheng, J. B. Tan, S. L. Cai, J. Fan and X. Yan, *J. Chromatogr. A*, 2013, **1285**, 132–138.
69 D. Bradshaw, J. B. Claridge, E. J. Cussen, T. J. Prior and M. J. Rosseinsky, *Acc. Chem. Res.*, 2005, **38**(4), 273–282.
70 Y. Liu, W. Xuan and Y. Cui, *Adv. Mater.*, 2010, **22**(37), 4112–4135.
71 X. J. Hu, G. Huang, S. Zhang, Z. B. Fang, T. F. Liu and R. Cao, *Chem. Commun.*, 2020, **56**(54), 7459–7462.
72 P. B. Rallapalli, M. C. Raj, S. Senthilkumar, R. S. Somani and H. C. Bajaj, *Environ. Prog. Sustainable Energy*, 2016, **35**(2), 461–468.
73 D. Jiang, L. L. Keenan, A. D. Burrows and K. J. Edler, *Chem. Commun.*, 2012, **48**(99), 12053–12055.
74 J. Bonnefoy, J. Canivet, D. Farrusseng, and Q. Alessandra, in *Inter. Symp. Nonporous Materials 7 (Nano7)*, 2014.
75 S. Yuan, W. Lu, Y. P. Chen, Q. Zhang, T. F. Liu, D. Feng and H. C. Zhou, *J. Am. Chem. Soc.*, 2015, **137**(9), 3177–3180.
76 X. Hou, T. Xu, Y. Wang, S. Liu, J. Tong and B. Liu, *ACS Appl. Mater. Interfaces*, 2017, **9**(37), 32264–32269.
77 L. Zhang and J. Jiang, *J. Membr. Sci.*, 2011, **367**(1–2), 63–70.
78 S. C. Xiang, Z. Zhang, C. G. Zhao, K. Hong, X. Zhao, D. R. Ding and B. Chen, *Nat. Commun.*, 2011, **2**(1), 1–7.
79 C. E. Dalgliesh, *J. Chem. Soc.*, 1952, 3940–3942.
80 V. A. Davankov, *Chirality*, 1997, **9**(2), 99–102.
81 M. Banerjee, S. Das, M. Yoon, H. J. Choi, M. H. Hyun and S. M. Park, *J. Am. Chem. Soc.*, 2009, **131**(22), 7524–7525.